Single-attosecond pulse generation with an intense multicycle driving pulse

Wei Cao,[1,2] Peixiang Lu,[1,2,*] Pengfei Lan,[1,2] Xinlin Wang,[1,2] and Guang Yang[1,2]
[1]*State Key Laboratory of Laser Technology and Wuhan National Laboratory for Optoelectronics, Huazhong University of Science and Technology, Wuhan 430074, People's Republic of China*
[2]*School of Optoelectronics Science and Engineering, Huazhong University of Science and Technology, Wuhan 430074, People's Republic of China*
(Received 3 April 2006; published 20 December 2006)

Higher-order harmonic generation from strong laser-atom interaction in the multicycle regime is investigated using the Lewenstein model. While the peak intensity of the driving laser is oversaturated, the atom will be ionized completely during a few half optical cycles. The harmonic spectrum then reveals a continuous multiplateau structure in the cutoff region because of the ground state depletion. Each subplateau can be superposed to generate single attosecond pulse. Since the intensity of high-order harmonics from ion is comparable to that from atom if the peak intensity is super-intense, appropriate subplateau should be selected for single attosecond pulse generation. It is also shown that the nonadiabatic effect plays a crucial role in tuning the bandwidth of the subplateau.

DOI: 10.1103/PhysRevA.74.063821 PACS number(s): 42.65.Re, 42.65.Ky, 32.80.Fb

I. INTRODUCTION

Intense laser-atom interaction results in a variety of nonlinear phenomena. Higher-order harmonic generation (HHG), as a typical one, has attracted lots of attentions in recent years. This is because HHG has created a new source of XUV and soft x-ray radiation, coherent radiation with photon energies up to 500 eV have been observed [1,2]. Another fascinating application of HHG is attosecond pulse production. A typical HHG spectrum shows that with the increase of harmonic order, the signal intensities decrease drastically for the first few low orders, then the intensities remain almost constant for many orders to form a plateau, at last the intensity drops sharply for the highest orders, which is called the cutoff. The discrete nature and broad envelope spectrum of HHG implies its potential for generating attosecond pulse train [3]. It is a major experimental breakthrough when it was demonstrated that a train of 250 as pulses was produced from the harmonic emission [4]. However, to extract an isolated pulse from the pulse train remains a major challenge. Up to now, single attosecond pulse generation based on HHG can be split into two categories: few-cycle regime [5–7] and ellipticity-modulated regime [8–11]. The first category can be explained by the fact that the highest harmonic is generated at the peak intensity of the ultrashort laser pulse where the duration is less than half an optical cycle. The second one is due to the sensitivity of harmonic yield to the ellipticity of the laser field. Very recently, it was proved that using a pulse with the peak intensity high enough has the potential of generating single ultrashort pulse beyond the femtosecond barrier [12], this is the application of the harmonics to the nonlinear optics in the soft x-ray regime, but the driving pulse is rather short (sub-10-femtosecond).

The physical mechanism of HHG can be well explained by the three-step theory [13]. When atoms are exposed in an intense laser field, the electrons may be tunnelling ionized, after propagating in the laser field, they recombine with the cores and emit high-energy photons. The conversion efficiency of HHG is mainly determined by two paths well known as the long electron trajectory and the short electron trajectory. In the classical picture, HHG in the plateau region is generated by both trajectories corresponding to two attosecond pulses per half optical cycle, while only one path contributes to the cutoff region, which results in single attosecond pulse per half optical cycle. In general, the laser intensity is far below the saturated intensity so the influence of the ionization is slight. While the laser field is oversaturated, the atoms will be sharply ionized during a few half optical cycles, the remarkable depletion of the ground state will play an essential role in the modulation of atomic harmonic spectrum [14,15] and then can limit the emission time of high harmonics. This perspective has been mentioned by Lappas and A L'Huillier [18]. Nevertheless, the pump pulse they used has a trapezoidal shape with two cycles of linear turn-on, followed by two cycles of constant amplitude and then two cycles of linear turn-off, it shows dramatic nonadiabatic effect and is actually equivalent to an ultrashort pulse with a duration of two optical cycles (about 5 fs). Besides, with the increasing of the driving laser intensity, higher-order harmonic emission from ions become remarkable [16,17], and this has been ignored by others [7,18]. In this paper we investigate the temporal characteristics of high harmonics generated in a highlyionizing regime, a longer multicycle driving pulse with $\sin^2$ envelope is applied, and both the atomic and ionic harmonic spectra are considered. We show that single attosecond pulse can still be generated with longer multicycle laser pulse by superposing an appropriate area in the cutoff region, the influence of the harmonics from ions has been removed through the band selection. This is a unique method to control the temporal character of harmonics. The paper is organized as follows: In Sec. II, we introduce the numerical simulation method. In Sec. III, the results are presented and discussed. Section IV contains the conclusion.

*Author to whom correspondence should be addressed. Email address: lupeixiang@mail.hust.edu.cn

II. NUMERICAL MODEL

In our model we consider the single-atom response, then the Lewenstein model can be used to calculate the dipole moment of an atom in the nonadiabatic formula [19]:

$$\vec{r}(t) = i\int_0^\infty d\tau\left(\frac{\pi}{\varepsilon + i\tau/2}\right)^{3/2}\vec{d}^*[\vec{P}_s(t,\tau) - \vec{A}(t)]a^*(t)$$
$$\times\exp(-iS(\vec{P}_s,t,\tau)) \times \vec{E}(t-\tau)\cdot\vec{d}[\vec{P}_s(t,\tau)$$
$$-\vec{A}(t-\tau)]a(t-\tau) + \text{c.c.} \quad (1)$$

Here, $\vec{E}(t)$ is the electric field of the laser pulse, $\vec{A}(t)$ is its associated vector potential. ε is a positive regularization constant, $\vec{P}_s$ and $S(\vec{P},t,\tau)$ represent the canonical momentum and quasiclassical action, respectively. Their values are given by:

$$\vec{P}_s(t,\tau) = \int_{t-\tau}^{t} dt''\vec{A}(t'')/\tau, S(\vec{P}_s,t,\tau)$$
$$= I_p\tau - \frac{1}{2}\vec{P}_s^2(t,\tau)\tau + \frac{1}{2}\int_{t-\tau}^{t}\vec{A}^2(t'')dt'', \quad (2)$$

I_p is the ionization potential of the interest atom, in the case of the hydrogenlike ground states, the dipole matrix element for transitions from the ground state to a continuum state can be approximated by:

$$\vec{d}(\vec{P}) = i\frac{2^{7/2}}{\pi}\alpha^{5/4}\frac{\vec{P}}{(\vec{P}^2+\alpha)^3}, \quad (3)$$

where $\alpha=2I_p$, $a(t)$ in Eq. (1) represents the ground state amplitude:

$$a(t) = \exp\left[-\int_{-\infty}^{t} w(t')dt'\right], \quad (4)$$

$w(t')$ is the ionization rate, which is calculated by the ADK theory [20]:

$$w(t) = \omega_p|C_{n^*}|^2 G_{lm}\left(\frac{4\omega_p}{\omega_t}\right)^{2n^*-m-1}\exp\left(-\frac{4\omega_p}{3\omega_t}\right), \quad (5)$$

where

$$\omega_p = \frac{I_p}{\hbar}, \quad \omega_t = \frac{e|\vec{E}(t)|}{\sqrt{2m_eI_p}}, \quad n^* = \left(\frac{I_{ph}}{I_p}\right)^{1/2}, \quad (6)$$

$$G_{lm} = \frac{(2l+1)(l+|m|)!(2^{-|m|})}{|m|!(l-|m|)!}, \quad (7)$$

$$|C_{n^*}|^2 = \frac{2^{2n^*}}{n^*\Gamma(n^*+l^*+1)\Gamma(n^*-l^*)}, \quad (8)$$

I_{ph} is the ionization potential of hydrogen, l and m are azimuthal and magnetic quantum numbers, e and m_e are electron charge and mass, respectively. The effective quantum number l^* is given by $l^*=0$ for $l\ll n$ or $l^*=n^*-1$ otherwise.

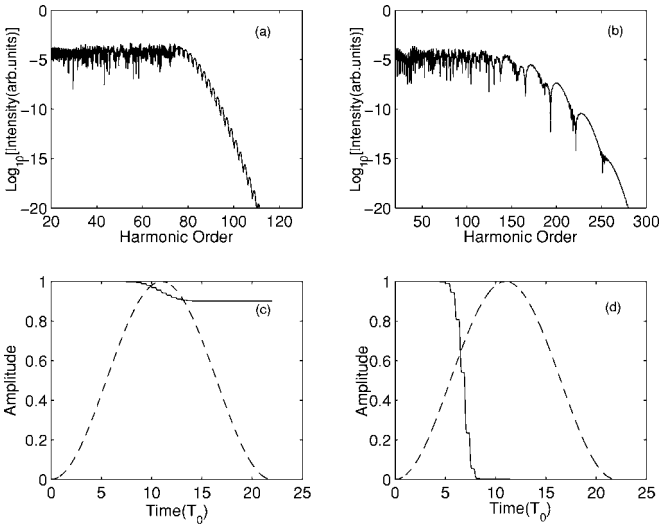

FIG. 1. Harmonic spectra (a), (b) and time history of the ground state amplitude [thin lines in (c),(d)] for neon illuminated by pulse with different peak intensities. (a)(c): 5×10^{14} W cm^{-2}; (b)(d): 2.5×10^{15} W cm^{-2}. The dashed lines in (c) and (d) denote the envelope of the laser pulse normalized by the peak intensity. T_0 is the optical cycle of the driven laser, which is 2.67 fs in our condition.

We use atomic units for all the calculations in this paper, where $\hbar=e=m_e=1$.

The harmonic amplitude $\mathbf{a}_q$ is obtained by Fourier transforming the time-dependent dipole acceleration $\mathbf{a}(t)$:

$$\mathbf{a}_q = \frac{1}{T}\int_0^T \mathbf{a}(t)\exp(-iq\omega t)dt, \quad (9)$$

where $\mathbf{a}(t)=\vec{r}(t)$, T and ω are the duration and frequency of the fundamental pulse, respectively. q corresponds to the harmonic order.

III. RESULTS AND DISCUSSION

The laser pulse in the calculation is described by $E(t)=E_0\sin(t\pi/T)^2\cos(\omega t+\phi_0)$, where ϕ_0 is the carrier-envelope phase, and E_0 denotes the maximum field strength of the laser pulse, T defines the pulse duration which is $\left(1-2\frac{\sin^{-1}(1/2)^{1/4}}{\pi}\right)T$. Here we choose Neon exposed to a laser pulse with the duration of 21.3 fs at 800 nm for the calculation, and the carrier-envelope phase is zero. Figure 1 shows the harmonic spectra and the time dependence of the population of the ground state for different laser intensities. At the peak intensity of 5×10^{14} W cm^{-2}, as shown in Figs. 1(a) and 1(c), only a small fraction of bound electrons, i.e., less than 10%, are ionized during the laser pulse, then the depletion of the ground state can be neglected. The harmonic spectrum shows a typical plateau-cutoff structure. When the peak intensity is increased to 2.5×10^{15} W cm^{-2}, as shown in Figs. 1(b) and 1(d), the atomic neon is deeply ionized, which results in a multiplateau structure near the cutoff region of the harmonic spectrum. The similar subplateau structure in HHG has been reported before [21,22]. The subplateaus in Ref. [21] are caused by different mechanisms of harmonics

generation from ion-atom collisions. In Ref. [22], the ionization probability provides information on the efficiency of the harmonics emission and forms the subplateau. However, in the case of Fig. 1(b), the multiplateau structure near the cutoff region of the spectrum can be explained by the ladder shape of the ground state amplitude [see Fig. 1(d)]. The probability amplitude of high harmonic field is determined by the three probability amplitudes assigned to each step [23], the most influential factor among them is the recombination amplitude [24], which corresponds to the interference of the ground and free states of the electron. As shown in Fig. 1(d), the ground state decays rapidly each half optical cycle near the saturated intensity. On the other hand, in the multicycle regime the laser amplitude increases slightly within half optical cycle, and then the ionization probability near the saturated intensity varies slowly with the laser intensity increasing. As a result, the ionization effect on the emission efficiency becomes less important than the ground state depletion. The efficiency of harmonics generation due to the interference of the ground and the free states of the electron will decrease each half optical cycle as the laser amplitude increases near the saturated intensity. In addition, the harmonic frequency is determined by the electrons' kinetic energy at the recombination time. Higher order harmonics are generated at higher intensities of the laser field. The harmonic spectrum then reveals a multiplateau structure near the cutoff region and the multiplateau structure corresponds to the ladder shape of the ground state amplitude near the saturated intensity. The cutoff region shows both smooth and regular features in the higher intensity case [Fig. 1(b)]. Each of the subplateaus is expanded to a continuous structure, and this indicates a better potential for ultrashort pulse generation in comparison with the modest intensity case [Fig. 1(a)]. The broadening of each subplateau is caused by the nonadiabatic effect of the laser field and the depletion of the ground state during each half optical cycle, these effects produce a linear frequency chirp. Another feature of the harmonic spectrum in Fig. 1(b) is that the cutoff location shifts from the cutoff law:

$$\hbar\omega_{\text{cutoff}} = I_p + 3.17U_p, \tag{10}$$

where $U_p = \frac{E^2}{4\omega^2}$ is the so-called ponderomotive potential in an oscillating field with a peak intensity of E and ω_{cutoff} represents the frequency of the emitted photon with the maximum energy. Because the atom has been completely ionized before the laser reaches its peak intensity, the cutoff location of the HHG spectrum is determined by the saturated intensity of the interest atom rather than the peak intensity of the exciting laser.

The time dependence of the superposition of harmonics in the cutoff region is shown in Fig. 2. At the modest intensity of 5×10^{14} W cm^{-2}, a train of attosecond pulses spaced by the half period $T_0/2$ of the driving field is generated in the cutoff region $80-100\omega$ [see Fig. 2(a)] each pulse is emitted near the peak of a half cycle. While the peak intensity of the laser field is increased to a higher value of 2.5×10^{15} W cm^{-2}, as shown in Fig. 2(b), the superposition of the first subplateau in the band between 141ω and 151ω generates a twin pulse. The first peak is approximately two

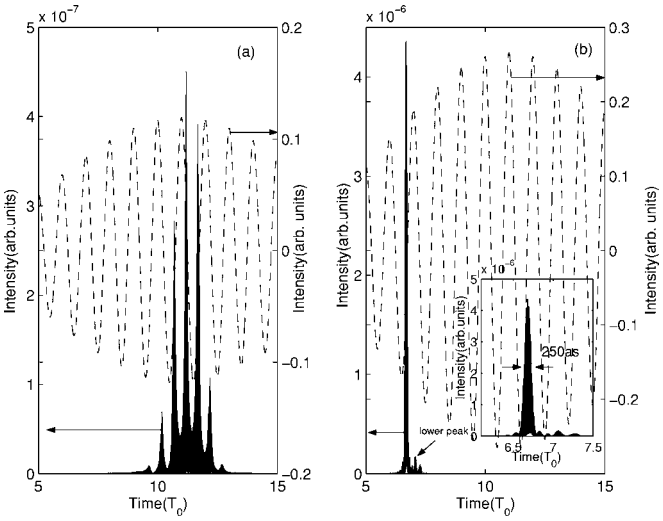

FIG. 2. (a) Time dependence of the superposition of harmonics $80-100\omega$ in Fig. 1(a) solid line) and the corresponding laser field (dashed line). (b) Time dependence of the superposition of harmonics $142-151\omega$ in Fig. 1(b) solid line) and the corresponding laser field (dashed line). The inset shows the details of the time profile of the radiation.

orders of magnitude higher than the second one, the inset in Fig. 2(b) shows its details. The two peaks of the twin pulse is separated by half oscillating period of the driving field which corresponds to the classical recollision time in the corkum model [13]. Then the profile of the radiation can be considered as a single attosecond pulse with a duration of 250 as. The minimum in the band 141ω occurs when the amplitude of the laser field increases to 0.16. At this amplitude, the atomic neon is seriously ionized with a period of $T_0/2$ [see Fig. 1(d)], which consists with the periodic depletion of the ground state amplitude. Harmonics in the cutoff region are generated within a few half optical cycles. While we neglect the ground state depletion, attosecond pulse train with each subpulse generated near the peak of each half optical cycle can be obtained in this region. In fact, the recombination process in HHG experiences a successive depletion of the ground state, then the following subpulses generated at higher intensities will be suppressed, only a twin pulse can be seen consequently. Each subplateau in the cutoff region of the spectrum in Fig. 1(b) has a continuous structure and thus can be superposed to generate a single attosecond pulse.

In order to obtain a better comprehension of the process. We make a time-frequency analysis on the dipole acceleration, the result as a spectrotemporal plot is shown in Fig. 3. The bows in Fig. 3 are produced when the electron moving along its classical trajectory returns to the atom. The ascending and descending arms of each bow correspond to the short and long trajectory, respectively. Then two subpulses happen during each half cycle of the laser field. At the top of each bow there is only one electron trajectory corresponding to a single pulse. The harmonic intensity is much weaker after the time $6.7T_0$ because of the deep ionization of the ground state, then if we select the appropriate subplateau, e.g. $141-151\omega$ in our case, a sequence of ultrashort radiation pulses separated by half oscillating cycle is generated. The first pulse

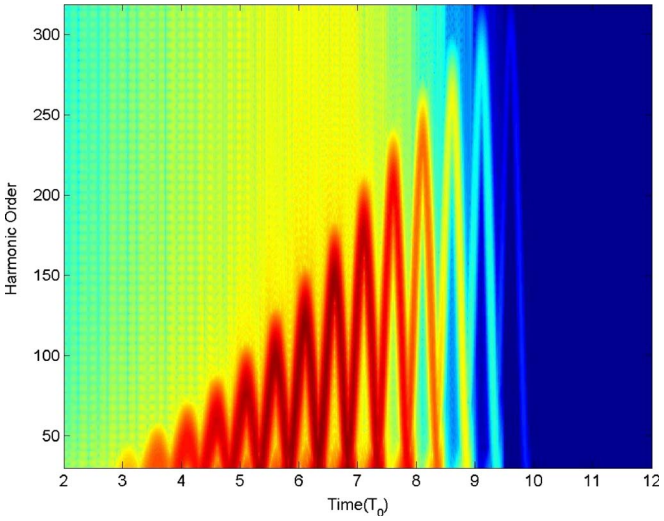

FIG. 3. (Color online) Spectral intensity vs time of harmonic radiation, the parameters are the same as in Fig. 1(a).

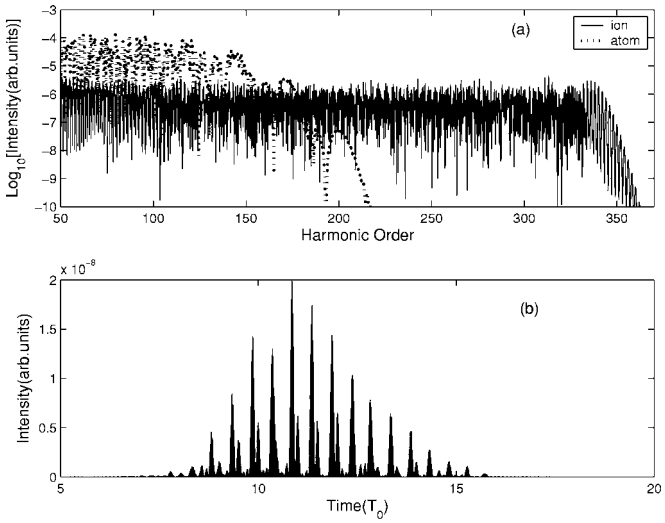

FIG. 4. (a) Harmonic spectra from Ne (dotted line) and Ne^+ (solid line), the parameters are the same as in Fig. 1. (b) Time profile of emission of the bands between 141ω to 151ω from harmonic spectrum of Ne^+.

happens at the top of the bow at about $6.7T_0$, and the subsequent radiation pulses with a much lower intensity are obtained around the middle of the subsequent bows, which indicates that each of the subsequent pulses has a crescent shape [see the inset of Fig. 2(b)]. Because of the successive degression of the pulse train, it results in a twin pulse with one peak much higher than the other, as shown in Fig. 2(b).

One important question to address is if the production of harmonic generation from the Ne ion could affect the results presented above. HHG from atom and ion in superintense pulsed laser field have been investigated by others [15,23], it is shown that the contribution to the high-energy HHG from ions precede over the atoms when the laser intensity is oversaturated. In our condition the laser intensity is above the saturation intensity for atomic neon, then the higher energy harmonic photons are mainly generated from the ionized neon. Figure 4(a) shows the harmonic spectra from Ne^+ (solid line) and Ne (dotted line), Fig. 4(b) is the time profile of the radiation of the band between 141ω and 151ω from Ne^+. We can see that in the lower-order part ($<$151 st harmonic), the harmonic yield intensity from atom Ne are about two orders of magnitude higher than that from Ne^+, while for higher order harmonics ($>$151 st harmonic), the intensity drops rapidly by many orders of magnitude for neon neutral due to the complete ionization. Nevertheless, the harmonic yield of Ne^+ is extended to about 350ω with almost the same intensity. To eliminate the effect of harmonics from Ne^+, we chose the first subplateau with the band of $141-151\omega$, where the contribution from Ne^+ can be neglected, the radiation emitted from the Ne^+ are about two orders of magnitude lower than that from atomic Ne [Fig. 4(b)]. Therefore, single attosecond pulse generation is not available in the following region ($>$151 st harmonic) because of the effect of the harmonics from ion.

If the peak intensity of the driving laser field was further increased, the nonadiabatic effect will become more remarkable. It is helpful for the broadening and regularity of the harmonic spectrum from atom, which will benefit the generation of single attosecond pulse. Figure 5 shows the harmonic signals from Ne atom with different peak intensities of the laser pulse. While the driving pulse intensity is higher, e.g., 6×10^{15} W cm^{-2}, the subplateaus of the harmonic spectrum are broadened in comparison with that in the lower intensity case. Then the band from 131ω to 161ω can be superposed to produce single attosecond pulse.

Another scheme of increasing the nonadiabatic degree of the laser pulse is to reduce the duration of the laser pulse. Figure 6(a) shows the harmonic spectrum from Ne atom exposed in a 5 fs laser pulse with a peak intensity of 4×10^{15} W cm^{-2}. Because the nonadiabatic degree is increased dramatically, the harmonic photons display a smooth, unmodulated spectrum up to the cutoff energy. Considering the decay of the ground state, we superpose the band of $51\omega-151\omega$ in order to eliminate the effect from ionic

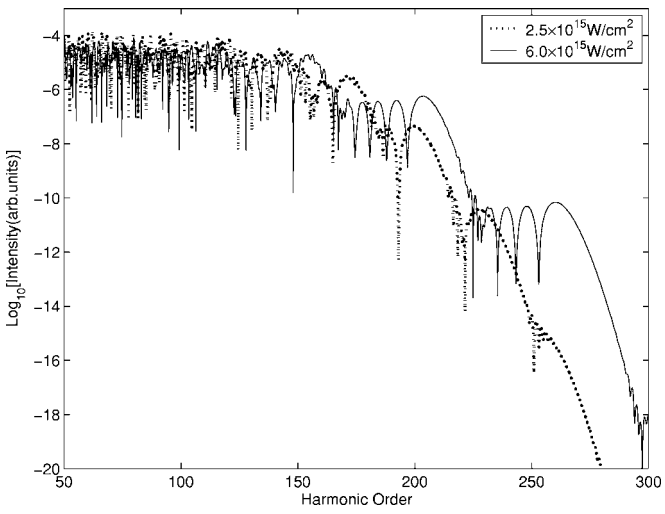

FIG. 5. Harmonic spectra from different peak intensities of the laser pulse, the peak intensities are 2.5×10^{15} W cm^{-2} (dotted line) and 6×10^{15} W cm^{-2} (thin line). The other parameters are the same as in Fig. 1(a).

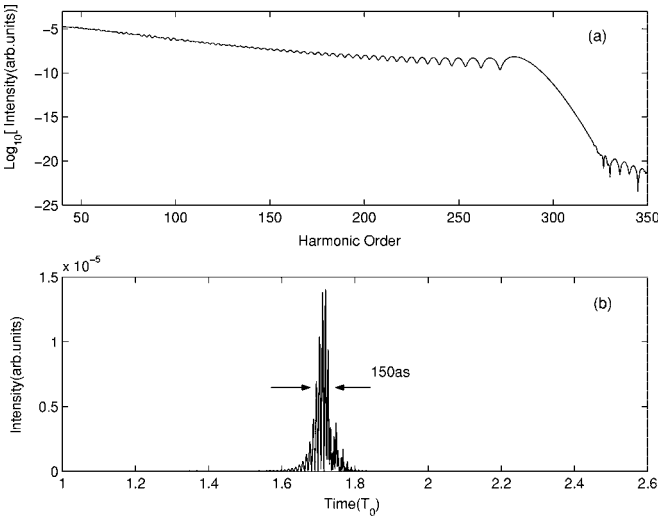

FIG. 6. (a) Harmonic spectra from Ne atom exposed in a laser pulse with the duration of 5 fs at a peak intensity of 4×10^{15} W cm^{-2}. (b) Time dependence of the superposition of harmonics $51-151\omega$.

harmonic, and obtain a single attosecond pulse with a duration of about 150 as [as shown in Fig. 6(b)]. This is rather similar with the result in Ref. [18]. Although the authors in Ref. [18] clarify that the whole plateau region has a potential for single subfemtosecond pulse generation in the over-the-barrier ionization (OBI) case, the driving pulse they used has a trapezoidal shape with two cycles of linear turn-on, followed by two cycles of constant amplitude and then two cycles of linear turn-off. The turn-on part of the pulse is rather abrupt in the OBI regime, this brings a high degree of nonadiabatic effect. The atom has been completely ionized before the peak intensity is reached, so the harmonic spectrum is independent of the constant part of the trapezoidal pulse, and the scheme is actually much equivalent to the few-cycle regime in Fig. 6. The bandwidth of each subplateau in the cutoff region depends on the nonadiabatic effect of the driven laser pulse, the more remarkable the nonadiabatic effect is, the broader the bandwidth will be. This indicates that single attosecond pulse can be produced using a driving pulse with an even longer duration, and increasing the peak intensity of the laser field can tune the bandwidth of the subplateau selected and improve the attosecond pulse generation. An important question which must be addressed is whether the single-atom picture is still applied when macroscopic responses are considered. At the highly ionizing regime, many free elections will be present in the laser focus. The ionization-induced plasma may distort the fundamental field and hence affect the quality of the harmonic pulses. However, single attosecond pulse generation can be still produced when proper experimental parameters were selected. For example, the propagation effects can be weakened by using thin gas medium at a low pressure. The volume effects can be eliminated by using loosely focused laser and thin gas jet [25]. In such case, the harmonic pulses still retain the features of a single atom and the scheme is feasible in experiment. A more complicated case considering a longer interaction medium to enhance the harmonic pulse brightness will be investigated in our future work.

IV. CONCLUSIONS

The harmonic generation from atom driven by a multicycle super-intense laser pulse has been investigated using the Lewenstein model. The numerical simulation demonstrates that a continuous multiplateau structure occurs in the cutoff region of the harmonic spectrum. Single attosecond pulse can be generated from the superposition of each subplateau. Considering the effect of harmonics from ion, appropriate subplateau should be selected. With the increasing of the nonadiabatic effect the subplateau will be broadened, this will benefit the generation of single attosecond pulse. Although the simulation results present the ideal single-atom response, the scheme is feasible in experiment while thin gas at a low pressure and laser system with long confocal parameters are chosen. To enhance the conversion efficiency, the optimization of more complicated experimental parameters will be investigated in future work.

ACKNOWLEDGMENTS

This work was supported by the National Natural Science Foundation of China under Grant No. 10574050, the Specialized Research Fund for the Doctoral Program of Higher Education of China under Grant No. 20040487023, and the National Basic Research Program of China under Grant No. 2006CB806006.

[1] Z. H. Chang *et al.*, Phys. Rev. Lett. **79**, 2967 (1997).
[2] C. Spielmann *et al.*, Science **278**, 661 (1997).
[3] P. Antoine, A. L'Huillier, and M. Lewenstein, Phys. Rev. Lett. **77**, 1234 (1996).
[4] P. M. Paul *et al.*, Science **292**, 1689 (2001).
[5] M. Hentschel *et al.*, Nature (London) **414**, 509 (2001).
[6] I. P. Christov, M. M. Murnane, and H. C. Kapteyn, Phys. Rev. Lett. **78**, 1251 (1997).
[7] F. Le Kien, K. Midorikawa, and A. Suda, Phys. Rev. A **58**, 3311 (1998).
[8] P. B. Corkum, N. H. Burnett, and M. Y. Ivanov, Opt. Lett. **19**, 1870 (1994).
[9] M. Ivanov, P. B. Corkum, T. Zuo, and A. Bandrauk, Phys. Rev. Lett. **74**, 2933 (1995).
[10] Z. Chang, Phys. Rev. A **70**, 043802 (2004).
[11] V. T. Platonenko and V. V. Strelkov, J. Opt. Soc. Am. B **16**, 435 (1998).
[12] T. Sekikawa, A. Kosuge, T. Kanai, and S. Watanabe, Nature (London) **432**, 605 (2004).
[13] P. B. Corkum, Phys. Rev. Lett. **71**, 1994 (1993).
[14] A. Sanpera, P. Jonsson, J. B. Watson, and K. Burnett, Phys. Rev. A **51**, 3148 (1995).
[15] S. C. Rae, K. Burnett, and J. Cooper, Phys. Rev. A **50**, 3438 (1994).

[16] E. A. Gibson, A. Paul, N. Wagner, R. Tobey, S. Backus, I. P. Christov, and M. M. Murnane, Phys. Rev. Lett. **92**, 033001 (2004).
[17] J. J. Carrera, Shih-I. Chu, and X. M. Tong, Phys. Rev. A **71**, 063813 (2005).
[18] D. G. Lappas and A. L'Huillier, Phys. Rev. A **58**, 4140 (1998).
[19] M. Lewenstein, P. Balcou, M. Y. Ivanov, A. L'Huillier, and P. B. Corkum, Phys. Rev. A **49**, 2117 (1994).
[20] M. V. Ammesov, N. B. Delone, and V. P. Krainov, Zh. Eksp. Teor. Fiz. **64**, 1191 (1986).
[21] M. Lein and J. M. Rost, Phys. Rev. Lett. **91**, 243901 (2003).
[22] A. de Bohan, P. Antoine, D. B. Milosevic, and B. Piraux, Phys. Rev. Lett. **81**, 1837 (1998).
[23] M. Y. Ivanov, T. Brabec, and N. Burnett, Phys. Rev. A **54**, 742 (1996).
[24] J. Itatani *et al.*, Nature (London) **432**, 867 (2004).
[25] I. P. Christov, M. M. Murnane, and H. C. Kapteyn, Phys. Rev. A **57**, R2285 (1998).